LARGE DEFORMATION WINDING MODELS

By

C. Mollamahmutoglu and J. K. Good
Oklahoma State University
USA

ABSTRACT

Almost all winding models incorporate the assumption of small linear deformations and strain in development. As such these models treat the addition of a layer of web to a winding roll with linear analysis using linear strain theory. Some webs such as tissues and nonwovens are highly extensible in-plane and highly compressible through their thickness. Do the models which assume small deformations apply to these web materials?

In this paper a winding model developed using large deformation theory will be presented. The output of this model will be compared with the results of winding tests done in the laboratory and with the outputs of models which employ small deformation theory to answer the question posed.

INTRODUCTION

Material characteristics of webs play an important role on the final state of the wound rolls. Among other parameters which are dictating hardness of the roll, the radial compressibility of the web dramatically affects the physical state of the wound roll by controlling the radial pressures. Radial pressures between layers should be low enough to avoid material damage and collapse but also they must be high enough to maintain wound roll structural integrity and stability. Thus a precise knowledge of pressures is important. [5]

Most web materials exhibit nonlinear characteristics in the radial direction. Material models incorporate this nonlinearity by defining radial modulus of elasticity dependent on radial pressure. One of the most widely accepted model is Pfeiffer's [4]. He defined two material constants (K_1, K_2) to model the radial material response:

$$J_R = K_2(P_R + K_1) \qquad \{1\}$$

Here P_R and J_R are the radial pressure which is taken positive and the tangent radial modulus, respectively. As seen from expression {1} the initial modulus is given as the product K_1K_2 and the springiness is represented by K_2. As the parameters K_1 and K_2 increase the hardness/rigidity will also increase. Nonlinear material models have been used with the linear equilibrium laws of elasticity in the development of wound roll models [1]. These models solve for the final solution state in several piecewise linear increments. Often the number of increments is equal to the number of layers in the roll. The incremental solutions produce increments in stress, strain, and deformation in each layer due to the addition of the most recent layer to the winding roll. The increments in stress within each layer are used to update the total stress within each lap. The total pressure is then used to update the radial modulus J_R prior to the addition of the next layer and incremental solution. Within each incremental solution the radial modulus in each layer is assumed to remain constant.

Linear equilibrium laws are always written and solved using the initial configurations of a mechanical system. When displacements and/or strains are small this type of formulation will provide accurate results. Linear elasticity or the so called small strain assumptions are considered to be valid for strains up to 1%. When strains exceed this value it is generally accepted that the solution formulation must account for the deformation of the body. This type of problem requires special considerations and is generally called a geometrically nonlinear problem. This is because the final geometry or the configuration of the mechanical system is not known a priori. This final configuration or deformed state is an additional unknown of the problem along with the stresses.

Web materials with low K_1 and K_2 values exhibit significant radial compaction during winding. The total radial strain can exceed 1%. The winding tension in conjunction with web material parameters such as $J_R(K_1,K_2)$ will be key in determining the total strain levels in the web layers and hence when a nonlinear wound roll model will be required to obtain an accurate solution. In this study a simple and efficient finite element method which accounts for material nonlinearity as well as geometrical nonlinearity will be demonstrated. Existing approaches to the problem will be examined and finally the importance of the nonlinear wound roll models will be discussed.

HISTORY OF THE PROBLEM

Modeling the effect of compaction on the wound roll stress development began with the efforts of Good et al [2]. They found that, for soft web materials, the measured in-roll radial pressures were considerably lower than the stresses predicted by the well known Hakiel [1] model. Good et al argued that during winding the tension of the outer layer is decreased significantly because of the compressibility of the outside of the winding roll. They determined the 'lost tension' by estimating the radial deformation u of the outer roll surface during winding. The radial deformation is used to calculate a loss in tangential strain which was then used to calculate the winding tension loss. Finally they modified the outer boundary of the Hakiel winding model [1] by incorporating this lost tension:

$$\delta\sigma_r\big|_{r=s} = -\left(T_w\big|_{r=s} + \frac{u\big|_{r=s}}{s} J_\theta \right)\frac{h}{s} \qquad \{2\}$$

Here T_w is the web tension in the winder tension zone, u is the radial deformation of the roll surface and is always negative so there is always a decrease in outer layer's tension, s is the radius of the current outer lap of thickness h, and J_θ is the in-plane web modulus in

the machine direction. Good et al verified this model with experiments. This model was formed of two sub components. One component estimated the current radial deformation of the outer surface of the roll due to the addition of the most recent layer and the other component solved for the stress increments due to modified outer boundary condition {2}. These increments in stress were then used to update the total layer stresses and the layer material properties. Benson [3] unified these two separate features in a large deformation model. He proposed a continuum based large deformation formulation which simultaneously tracked the deformed shape of roll and calculated the in-roll stresses. One of the distinct features of his formulation was the use of new material constants. Benson employed different strain definitions which required him to employ different material constants (α , β) to define the radial modulus instead of Pfeiffer's constants (K_1, K_2). He did not propose a method to calculate his constants (α , β) based upon given values of Pfeiffer's constants (K_1, K_2). Benson verified his results by comparison to Good et al's pressure test data which also compared well with results from Good et al's tension loss model.

The models developed by Good et al and Benson were one dimensional. The output of one dimensional winding models are limited to radial and tangential stresses as a function of radius. Arola [6] was the first to extend large deformation calculations into a two dimensional winding model where stresses could vary both as a function of radius *r* and of CMD (*z*) location. He proposed a 2D large deformation model based on continuum mechanics. He solved the nonlinear equations using linearization and employing the finite element method. Arola produced results for the comparison with Hakiel's model. His large deformation model produced pressure results that were about 10% less than those yielded by Hakiel's small deformation model. He also compared his results to Benson's model but did not present the comparison. Arola reported that he got even better agreement with Benson's model which is logical given that the results from two large deformation models should agree better. Although Arola gave extensive detail in the formulation of the mathematical structure he did not mention how to select consistent material properties for his stress and strain measurements. Also he did not present details of how he treated the outer boundary condition for the winding roll.

Nonlinear formulations demand more in terms of computational time and since they generally use different strain definitions they also require different material models for consistency. In this study we propose an efficient and yet consistent model. Benson's nonlinear model and Arola's material model were coded for comparisons. Results from all codes are compared with winding experiments done on a spun-bond polypropylene non-woven web and on a bath tissue web which are much more compressible than the newsprint that Good et al wound in previous tests.

NONLINEAR GEOMETRIC FORMULATION

A one dimensional finite element will be developed which can model both geometric and material nonlinear behavior for axisymmetric wound roll analysis. The starting point of development is the virtual work expression. This can be stated as the equality of virtual internal and external works for all configurations:

$$\delta W_{\text{int}} = \delta W_{ext} \qquad \{3\}$$

For the current configuration the internal virtual work is the virtual work of the real or the Cauchy stress field acting through the virtual strains:

$$\delta W_{\text{int}} = \int_v \delta\varepsilon^T (\sigma \ - \sigma_0) dv \qquad \{4\}$$

Here $\delta\varepsilon$, σ , σ_0 are the virtual strain vector, the current Cauchy stress vector and the Cauchy counterpart of the initial stress vector, respectively. The integration is performed for the current configuration. The external virtual work the work of external forces acting through corresponding virtual displacements:

$$\delta W_{ext} = \int_v \delta u^T b \ dv + \int_a \delta u^T q \ da \qquad \{5\}$$

where *q* are the external distributed loads acting over the surface of an element and *b* is the body force component acting over the volume of the element. In nonlinear geometrical analysis there is a certain difference between the various configurations of the body. The deformation of the system must be accounted for and physical quantities must be defined according to the selected configuration. As mentioned above the virtual work expression {4}, {5} was written for the current configuration. Hence the stresses are Cauchy stresses and the strains are small displacement strain components which are the work conjugate of each other. One of the most common virtual work structures for the nonlinear finite element analysis is to write virtual work expression in terms of initial coordinates. Now the virtual work expressions can be converted to the following counterparts for the initial configuration:

$$\delta W_{\text{int}} = \int_V (S - S_0) : \delta E \ dV \qquad \{6a\}$$

$$\delta W_{\text{int}} = \int_V (P - P_0) : \delta F \ dV \qquad \{6b\}$$

$$\delta W_{ext} = \int_V \delta u^T B \ dV + \int_A \delta u^T Q \ dA \qquad \{7\}$$

Here the capital indexes denote that the quantity is written in terms of initial coordinates (i.e. *v* is for current and *V* is for initial volume). Generally there are two forms for the initial counterpart of the internal virtual work expression. During the first transformation {6b} from current to initial coordinates the Cauchy stresses (σ) are converted to 1st Piloa-Kirchoff stresses (*P*) and the small strains (ε) are converted into the deformation gradient (*F*). The second transformation {6a} converts the Cauchy stresses to the 2nd Piloa-Kirchoff stresses (*S*) and the small strains to Green-Lagrange strains (*E*). These two transformations are identical to each other but they have own advantages. For example while first transformation allows simpler numerical formulations the second protects symmetry in numerical formulations. In order to facilitate derivations, the internal work expression is now formed as an inner product of stress and strain tensors rather then the previous vector multiplication employed for the current configuration. Since the current configuration is unknown the virtual work expression is highly nonlinear in terms of displacements. In general it is impossible to find an analytical solution for the nonlinear virtual work expression so it is linearized in terms of

displacements and iterative techniques are employed. The linearization is carried out by means of a directional derivative which is based on a Taylor series expansion in multiple dimensions. Both the internal and external work may depend on the displacement field and also the constitutive relations may be nonlinear as in the example of web materials. Considering this the internal and external forces are written as a function of displacement field *u*:

$$\begin{aligned} \delta W_{int} &= \delta W_{int}(u) \\ \delta W_{ext} &= \delta W_{ext}(u) \end{aligned} \quad \{8\}$$

Taking the directional derivative of $\delta W_{\text{int}}(u)$ and $\delta W_{ext}(u)$ in the direction of *u* yields:

$$\delta W_{\text{int}} + D_{\Delta u}\delta W_{\text{int}} = \delta W_{ext} + D_{\Delta u}\delta W_{ext} \quad \{9\}$$

Here the directional derivative is given as:

$$D_{\Delta u}\delta W = \left.\frac{d\delta W(u+\lambda\Delta u)}{d\lambda}\right|_{\lambda=0} \quad \{10\}$$

After rearranging the virtual work expression, the linear form in terms of incremental displacement vector Δu is obtained:

$$D_{\Delta u}\delta W_{\text{int}} - D_{\Delta u}\delta W_{ext} = -\delta W_{\text{int}} + \delta W_{ext} \quad \{11\}$$

The right hand side is known for a given configuration (i.e. for a given field *u* it will be shown explicitly that the left hand side is linear in terms of unknown incremental displacement vector Δu). This can provide a solution for the incremental displacements and after updating the total displacements a new configuration can be calculated progressing toward the final configuration of mechanical system.

COMPACT AXISYMMETRICAL FORMULATION

The wound roll is assumed to be an axisymmetric body which is formed by the accumulation of the concentric hoops. In this formulation the concept of an initial stress will be employed. It will be assumed that the hoops/layers are initially stressed due to web line stress. This initial stress will be the only source of load. In this case the external virtual work will vanish and the general linearized form incorporating the directional derivative is:

$$D_{\Delta u}\delta W_{\text{int}} = -\delta W_{\text{int}} \quad \{12\}$$

Two nonlinear finite element models based on two different material models will be developed. These two models will share a common compact finite element formulation.

Model II

In the first model the material law proposed by Arola will be adopted which requires use of the first virtual work expression {6a}. The axisymmetric form of the first virtual work expression is:

$$\delta W_{\text{int}} = \int_A tr\left[(S - S_0).\delta E^T\right] RdRdZ \qquad \{13\}$$

In the expression the factor of 2π is excluded due to axisymmetry. A compact finite element formulation will be developed in which the wound roll is assumed to exist in plane strain conditions. This assumption dictates that CMD (z) direction strains and shear strains all vanish. In this case the Green Lagrange strain tensor takes the form:

$$E = \frac{1}{2}\begin{bmatrix} \left(\frac{\partial r}{\partial R}\right)^2 - 1 & 0 \\ 0 & \left(\frac{r}{R}\right)^2 - 1 \end{bmatrix} \qquad \{14\}$$

The variation of the Green Lagrange strain tensor with respect to the displacement field is:

$$\delta E = \begin{bmatrix} \delta\left(\frac{\partial r}{\partial R}\right)\frac{\partial r}{\partial R} & 0 \\ 0 & \delta\left(\frac{r}{R}\right)\frac{r}{R} \end{bmatrix} \qquad \{15\}$$

Since all the shear strains and CMD strains vanish, the only virtual work will be done by radial and tangential stresses and thus the stress tensor takes the following form:

$$S = \begin{bmatrix} S_R & 0 \\ 0 & S_\theta \end{bmatrix} \qquad \{16\}$$

The initial stress tensor will have only one nonzero component. The initial tangential stress component is equal to the negative web line stress ($-T_w$):

$$S_0 = \begin{bmatrix} 0 & 0 \\ 0 & -T_w \end{bmatrix} \qquad \{17\}$$

Now the variation of the internal energy {12} can be expressed as:

$$\delta W_{\text{int}} = \int_A \left(\frac{\partial r}{\partial R} S_R \delta\left(\frac{\partial r}{\partial R}\right) + \frac{r}{R}(S_\theta + T_w)\delta\left(\frac{r}{R}\right)\right) RdRdZ \qquad \{18\}$$

In the compact finite element formulation reduced quadrilateral elements have been employed with a unit thickness and as seen in Figures 1 and 2. A typical element has two degrees of freedom which include the radial displacements at the edges u_1 and u_2.

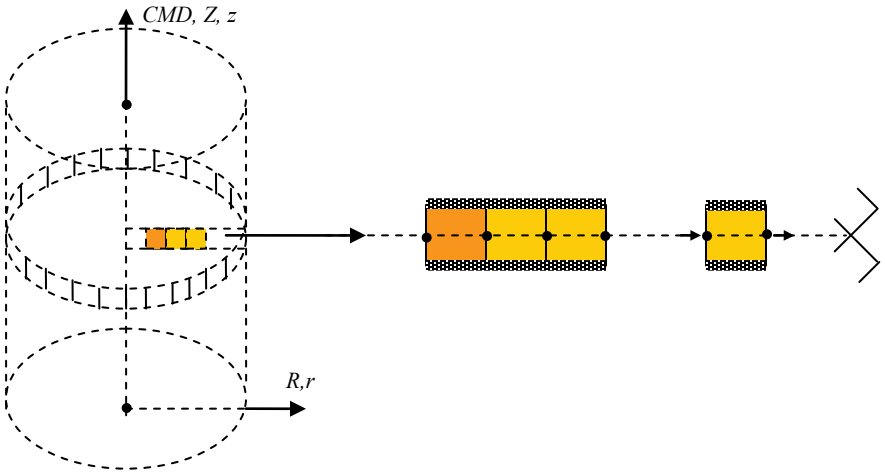

Figure 1 – The Axisymmetric Representation

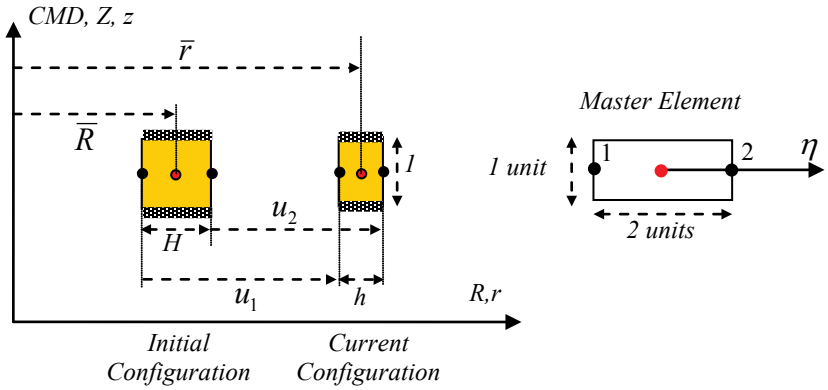

Figure 2 – The Compact Finite Element

An isoparametric formulation was implemented with the well-known shape functions:

$$u = u_1 \frac{1-\eta}{2} + u_2 \frac{1+\eta}{2} \qquad \{19\}$$

and thus the maps between the real coordinates and the natural coordinate η is:

$$R = \bar{R} + \eta \frac{H}{2} \qquad \{20\}$$

$$r = \bar{r} + \eta \frac{h}{2} \qquad \{21\}$$

where $\bar{r}$ and $\overline{R}$ are radial coordinates of the mid point of an element for the current and initial configurations, respectively. Similarly, as seen in Figure 2, *h* and *H* are the thicknesses of an element for the current and initial configurations, respectively. By employing the nodal displacements the geometric relations between initial and current configurations can be written as:

$$\bar{r} = \overline{R} + \frac{u_1 + u_2}{2} \qquad \{22\}$$

$$h = H + u_2 - u_1 \qquad \{23\}$$

Now the variation of the Green Lagrange strain components can be approximated as:

$$\frac{\partial r}{\partial R} = \frac{h}{H} \qquad \{24\}$$

$$\frac{r}{R} = \frac{2\bar{r} + \eta h}{2\overline{R} + \eta H} \qquad \{25\}$$

Inserting the above expressions into the variation of the internal energy {18}, accounting for the unit thickness and rearranging yields:

$$\delta W_{\text{int}} = \int_{-1}^{1} \left(\frac{h}{H} S_R \frac{(\delta u_2 - \delta u_1)}{H} + \frac{r}{R}(S_\theta + T_w) \frac{\delta u_2 + \delta u_1 + \eta(\delta u_2 - \delta u_1)}{2R} \right) R \frac{H}{2} d\eta \qquad \{26\}$$

Now the directional derivative can be incorporated directly by taking differentials of the stress components S_R and S_θ :

$$D_{\Delta u}\delta W_{\text{int}} = \int_{-1}^{1} \left(D_{\Delta u}(hS_R) \frac{(\delta u_2 - \delta u_1)}{H^2} + D_{\Delta u}(rS_\theta + rT_w) \frac{\delta u_2 + \delta u_1 + \eta(\delta u_2 - \delta u_1)}{2R^2} \right) R \frac{H}{2} d\eta \qquad \{27\}$$

The differentials for the directional derivative can be expressed as Taylor series expansions and if only the linear terms are retained:

$$D_{\Delta u}(hS_R) = \left(h \frac{\partial S_R}{\partial u_1} - S_R \right) \Delta u_1 + \left(h \frac{\partial S_R}{\partial u_2} + S_R \right) \Delta u_2 \qquad \{28a\}$$

$$D_{\Delta u}(rS_\theta + rT_w) = \left(r \frac{\partial S_\theta}{\partial u_1} + \frac{S_\theta + T_w}{2} \right) \Delta u_1 + \left(r \frac{\partial S_\theta}{\partial u_2} + \frac{S_\theta + T_w}{2} \right) \Delta u_2 \qquad \{28b\}$$

where the term $D_{\Delta u}T_w$ vanished because it is independent from the displacements and the expressions simplified because:

$$\partial h/\partial u_1 = -\partial h/\partial u_2 = -1 \qquad \{29a\}$$

$$\partial r/\partial u_1 = \partial r/\partial u_2 = 1/2 \qquad \{29b\}$$

Inserting differentials into expression {27} and rearranging produces the following linearized form of the virtual work expression in terms of the incremental displacements Δu_1, Δu_2:

$$\delta u_1 \left\{ \int_{-1}^{1} A_1 d\eta \right\} + \delta u_2 \left\{ \int_{-1}^{1} A_2 d\eta \right\} = 0 \qquad \{30\}$$

where

$$\begin{aligned} A_1 = &-\frac{R}{2H}\left(\left(h\frac{\partial S_R}{\partial u_1} - S_R\right)\Delta u_1 + \left(h\frac{\partial S_R}{\partial u_2} + S_R\right)\Delta u_2\right) \\ &+\frac{H(1-\eta)}{4R}\left(\left(r\frac{\partial S_\theta}{\partial u_1} + \frac{S_\theta + T_w}{2}\right)\Delta u_1 + \left(r\frac{\partial S_\theta}{\partial u_2} + \frac{S_\theta + T_w}{2}\right)\Delta u_2\right) \\ &-\frac{RhS_R}{2H} + \frac{rH(1-\eta)}{4R}(S_\theta + T_w) \end{aligned}$$

and

$$\begin{aligned} A_2 = &\frac{R}{2H}\left(\left(h\frac{\partial S_R}{\partial u_1} - S_R\right)\Delta u_1 + \left(h\frac{\partial S_R}{\partial u_2} + S_R\right)\Delta u_2\right) \\ &+\frac{H(1+\eta)}{4R}\left(\left(r\frac{\partial S_\theta}{\partial u_1} + \frac{S_\theta + T_w}{2}\right)\Delta u_1 + \left(r\frac{\partial S_\theta}{\partial u_2} + \frac{S_\theta + T_w}{2}\right)\Delta u_2\right) \\ &+\frac{RS_R}{2H} + \frac{rH(1+\eta)}{4R}(S_\theta + T_w) \end{aligned}$$

Since the virtual displacements are arbitrary and to satisfy the linearized form of virtual work it is required that:

$$\int_{-1}^{1} A_1 d\eta = 0 \qquad \{31a\}$$

$$\int_{-1}^{1} A_2 d\eta = 0 \qquad \{31b\}$$

If we rearrange again and use matrix notation we obtain element stiffness equations:

$$^{II}K^e \Delta u = {}^{II}F^e \qquad \{32\}$$

where:

$$ {}^{II}K_{11}^{e} = \int_{-1}^{1} -\frac{R}{2H}\left(h\frac{\partial S_R}{\partial u_1} - S_R \right) + \frac{H(1-\eta)}{4R}\left(r\frac{\partial S_\theta}{\partial u_1} + \frac{S_\theta + T_w}{2} \right) d\eta \qquad \{33a\} $$

$$ {}^{II}K_{22}^{e} = \int_{-1}^{1} \frac{R}{2H}\left(h\frac{\partial S_R}{\partial u_2} + S_R \right) + \frac{H(1+\eta)}{4R}\left(r\frac{\partial S_\theta}{\partial u_2} + \frac{S_\theta + T_w}{2} \right) d\eta \qquad \{33b\} $$

$$ {}^{II}K_{12}^{e} = \int_{-1}^{1} -\frac{R}{2H}\left(h\frac{\partial S_R}{\partial u_2} + S_R \right) + \frac{H(1-\eta)}{4R}\left(r\frac{\partial S_\theta}{\partial u_2} + \frac{S_\theta + T_w}{2} \right) d\eta \qquad \{33c\} $$

$$ {}^{II}K_{21}^{e} = \int_{-1}^{1} \frac{R}{2H}\left(h\frac{\partial S_R}{\partial u_1} - S_R \right) + \frac{H(1+\eta)}{4R}\left(r\frac{\partial S_\theta}{\partial u_1} + \frac{S_\theta + T_w}{2} \right) d\eta \qquad \{33d\} $$

$$ {}^{II}F_{1}^{e} = \frac{RhS_R}{2H} - \frac{rH(1-\eta)}{4R}(S_\theta + T_w) \qquad \{34a\} $$

$$ {}^{II}F_{2}^{e} = -\frac{RhS_R}{2H} - \frac{rH(1+\eta)}{4R}(S_\theta + T_w) \qquad \{34b\} $$

and $\Delta u = \begin{bmatrix} \Delta u_1 & \Delta u_2 \end{bmatrix}^T$.

Here ${}^{II}K^e$ and ${}^{II}F^e$ are the 2x2 element tangent stiffness matrix and the load vector, respectively. The left superscript *II* indicates that the quantities are derived for 2nd Piola Kirchoff stresses. Now the finite element formulation is ready to implement a material model. The first material model which will be employed is due to Arola. Here a simplified version of Arola's model will be employed which is suitable for plane analysis. Furthermore the Poisson ratios other than the in-plane ratios are omitted because they are reported to be small in the literature. Arola never mentioned it explicitly but as seen from his formulations and calculations he assumed a constitutive law which relates the 2nd Piola Kirchoff stresses and Green Lagrange strains identical to small strain theory. Thus Arola's radial material model directly comes from Pfeiffer:

$$ S_R = K_1(1 - \exp(-K_2 E_R)) \qquad \{35a\} $$

The plane strain counterpart (with only nonzero in-plane Poisson ratio) of his tangential material model is:

$$ S_\theta = \frac{J_\theta J_{CMD}}{J_{CMD} - J_\theta \nu_{CMD\theta}^2}(E_\theta) \qquad \{35b\} $$

where J_θ, J_{CMD} and $\nu_{CMD\theta}$ are the tangential and CMD modulus of elasticity and the in-plane Poisson ratio, respectively, and they are measured using nominal stresses and linear strains. K_1 and K_2 are Pfeiffer's constants. Although using small strain constants with Green Lagrange strains is inconsistent the material model will be used for comparison.

The material model can be written explicitly in terms of nodal displacements by using the definitions of the Green Lagrange strains:

$$E_R = \frac{1}{2}\left(\left(\frac{H + u_2 - u_1}{H}\right)^2 - 1\right) \qquad \{36a\}$$

$$E_\theta = \frac{1}{2}\left(\left(\frac{2R + u_2 + u_1 + (u_2 - u_1)\eta}{2R}\right)^2 - 1\right) \qquad \{36b\}$$

Using the chain rule and taking derivatives of the stresses with respect to the nodal yields:

$$\frac{\partial S_R}{\partial u_1} = -\frac{\partial S_R}{\partial u_2} = -{}^{II}J_R \frac{h}{H^2} \qquad \{37a\}$$

$$\frac{\partial S_\theta}{\partial u_1} = \frac{\partial S_\theta}{\partial u_2} = J_\theta^* \frac{r}{2R^2} \qquad \{37b\}$$

where:

$${}^{II}J_R = K_2(K_1 - S_R)$$

$$J_\theta^* = \frac{J_\theta J_{CMD}}{J_{CMD} - J_\theta \nu_{CMD\theta}^2}$$

Inserting these derivatives {37} into the stiffness terms {33} and integrating will complete the complete nonlinear finite element formulation of a typical element. If constant strain is assumed throughout the element and thus after setting $\eta = 0$ the following simplified form for the element tangent stiffness matrix and element force vector is obtained:

$${}^{II}K^e = \begin{bmatrix} \frac{R}{H}\left(\frac{{}^{II}J_R h^2}{H^2} + S_R\right) + \frac{H}{2R}\left(\frac{J_\theta^* r^2}{2R^2} + \frac{S_\theta + T_w}{2}\right) & -\frac{R}{H}\left(\frac{{}^{II}J_R h^2}{H^2} + S_R\right) + \frac{H}{2R}\left(\frac{J_\theta^* r^2}{2R^2} + \frac{S_\theta + T_w}{2}\right) \\ \textit{sym.} & \frac{R}{H}\left(\frac{{}^{II}J_R h^2}{H^2} + S_R\right) + \frac{H}{2R}\left(\frac{J_\theta^* r^2}{2R^2} + \frac{S_\theta + T_w}{2}\right) \end{bmatrix}$$

$${}^{II}F^e = \begin{bmatrix} \frac{Rh}{H} S_R - \frac{Hr}{2R}(S_\theta + T_w) \\ -\frac{Rh}{H} S_R - \frac{Hr}{2R}(S_\theta + T_w) \end{bmatrix}$$

Model I

The second formulation, which uses a different material model, begins with the second virtual work expression {6b} which in an axisymmetric form is:

$$\delta W_{\text{int}} = \int_A tr\left[(P - P_0).\delta F^T\right] RdRdZ \qquad \{38\}$$

The plane strain assumption dictates that CMD direction strains and shear strains all vanish as previously and in this case the deformation gradient tensor simplifies to:

$$F = \begin{bmatrix} \left(\frac{\partial r}{\partial R}\right) & 0 \\ 0 & \left(\frac{r}{R}\right) \end{bmatrix} \qquad \{39\}$$

Taking the variation with respect to displacement field yields the variation of deformation gradient tensor:

$$\delta F = \begin{bmatrix} \delta\left(\frac{\partial r}{\partial R}\right) & 0 \\ 0 & \delta\left(\frac{r}{R}\right) \end{bmatrix} \qquad \{40\}$$

Again in the case of plane strain all shear strains and CMD strains vanish and the virtual work will be done only by the radial and tangential stresses. Thus the 1st Piola Kirchoff stress tensor takes the following simplified form:

$$P = \begin{bmatrix} P_R & 0 \\ 0 & P_\theta \end{bmatrix} \qquad \{41\}$$

As before, the initial stress tensor will have only one nonzero component: the initial tangential stress component which is directly equal to negative of web line stress $-T_w$:

$$P_0 = \begin{bmatrix} 0 & 0 \\ 0 & -T_w \end{bmatrix} \qquad \{42\}$$

Now the inner product of variation of internal energy in expression {38} can be expanded:

$$\delta W_{\text{int}} = \int_A \left(P_R \delta\left(\frac{\partial r}{\partial R}\right) + (P_\theta + T_w)\delta\left(\frac{r}{R}\right)\right) RdRdZ \qquad \{43\}$$

Employing the same isoparametric formulation the following expression for the variation of the virtual work is produced:

$$\delta W_{\text{int}} = \int_{-1}^{1} \left(P_R \frac{(\delta u_2 - \delta u_1)}{H} + (P_\theta + T_w)\frac{\delta u_2 + \delta u_1 + \eta(\delta u_2 - \delta u_1)}{2R}\right) R\frac{H}{2} d\eta \qquad \{44\}$$

Linearization will be carried out similarly to the first formulation. Derivatives are taken with respect to nodal displacements and only the linear terms are retained:

$$D_{\Delta u}\delta W_{\text{int}} = \int_{-1}^{1}\left(D_{\Delta u}(P_R)\frac{(\delta u_2 - \delta u_1)}{H} + D_{\Delta u}(P_\theta + T_w)\frac{\delta u_2 + \delta u_1 + \eta(\delta u_2 - \delta u_1)}{2R}\right)R\frac{H}{2}d\eta \quad \{45\}$$

where

$$D_{\Delta u}(P_R) = \frac{\partial P_R}{\partial u_1}\Delta u_1 + \frac{\partial P_R}{\partial u_2}\Delta u_2 \quad \{46a\}$$

and

$$D_{\Delta u}(P_\theta) = \frac{\partial P_\theta}{\partial u_1}\Delta u_1 + \frac{\partial P_\theta}{\partial u_2}\Delta u_2 \quad \{46b\}$$

Inserting these differentials and rearranging yields the following linearized form of the virtual work expression in terms of the incremental displacements Δu_1, Δu_2:

$$\delta u_1\left\{\int_{-1}^{1} B_1 d\eta\right\} + \delta u_2\left\{\int_{-1}^{1} B_2 d\eta\right\} = 0 \quad \{47\}$$

where

$$B_1 = -\frac{R}{2}\left(\frac{\partial P_R}{\partial u_1}\Delta u_1 + \frac{\partial P_R}{\partial u_2}\Delta u_2\right) + \frac{H(1-\eta)}{4}\left(\frac{\partial P_\theta}{\partial u_1}\Delta u_1 + \frac{\partial P_\theta}{\partial u_2}\Delta u_2\right) - \frac{RP_R}{2} + (P_\theta + T_w)\frac{H(1-\eta)}{4}$$

$$B_2 = \frac{R}{2}\left(\frac{\partial P_R}{\partial u_1}\Delta u_1 + \frac{\partial P_R}{\partial u_2}\Delta u_2\right) + \frac{H(1+\eta)}{4}\left(\frac{\partial P_\theta}{\partial u_1}\Delta u_1 + \frac{\partial P_\theta}{\partial u_2}\Delta u_2\right) + \frac{RP_R}{2} + (P_\theta + T_w)\frac{H(1+\eta)}{4}$$

Invoking the principle of virtual work it can be concluded:

$$\int_{-1}^{1} B_1 d\eta = 0 \quad \{48a\}$$

$$\int_{-1}^{1} B_2 d\eta = 0 \quad \{48b\}$$

These equations can be arranged in the matrix form as previously:

$${}^{I}K^{e}\Delta u = {}^{I}F^{e} \quad \{49\}$$

where:

$${}^{I}K_{11}^{e} = -\frac{R}{2}\frac{\partial P_R}{\partial u_1} + \frac{H(1-\eta)}{4}\frac{\partial P_\theta}{\partial u_1} \quad \{50a\}$$

$$ {}^{I}K^{e}_{22} = \frac{R}{2}\frac{\partial P_R}{\partial u_2} + \frac{H(1+\eta)}{4}\frac{\partial P_\theta}{\partial u_2} \quad \{50b\} $$

$$ {}^{I}K^{e}_{12} = -\frac{R}{2}\frac{\partial P_R}{\partial u_2} + \frac{H(1-\eta)}{4}\frac{\partial P_\theta}{\partial u_2} \quad \{50c\} $$

$$ {}^{I}K^{e}_{21} = \frac{R}{2}\frac{\partial P_R}{\partial u_1} + \frac{H(1+\eta)}{4}\frac{\partial P_\theta}{\partial u_1} \quad \{50d\} $$

and

$$ {}^{I}F^{e}_{1} = \frac{RP_R}{2} - (P_\theta + T_w)\frac{H(1-\eta)}{4} \quad \{51a\} $$

$$ {}^{I}F^{e}_{2} = -\frac{RP_R}{2} - (P_\theta + T_w)\frac{H(1+\eta)}{4} \quad \{51a\} $$

Here ${}^{I}K^{e}$, ${}^{I}F^{e}$ are the 2x2 element tangent stiffness matrix and the load vector, respectively. The left superscript *I* indicates that the quantities are derived for the 1st Piola Kirchoff stresses. The material model proposed uses the 1st Piola Kirchoff stresses and the linear strains. This is convenient because in the material characterization experiments (stack compression and MD modulus tests) the stresses are always calculated over initial dimensions of the specimens. Thus the stresses used to model material behavior are the nominal stresses or simply the 1st Piola Kirchoff stresses used in the analysis. The material model thus has become:

$$ P_R = K_1(1 - \exp(-K_2(F_R - 1))) \quad \{52a\} $$

$$ P_\theta = \frac{J_\theta J_{CMD}}{J_{CMD} - J_\theta \nu^2_{CMD\theta}}(F_\theta - 1) \quad \{52b\} $$

where K_1 and K_2 are Pfeiffer's constants, J_θ, J_{CMD} and $\nu_{CMD\theta}$ are the tangential and CMD modulus of elasticity and in-plane Poisson ratio, respectively. These material constants are measured with nominal stresses (here 1st Piola Kirchoff stresses) and linear strains. F_R and F_θ are the deformation gradient components for the radial and tangential direction, respectively, and they are simply related to the corresponding linear strain components ε_R and ε_θ:

$$ \varepsilon_R = F_R - 1 = \frac{u_2 - u_1}{H} \quad \{53a\} $$

$$ \varepsilon_\theta = F_\theta - 1 = \frac{u_2 + u_1 + (u_2 - u_1)\eta}{2R} \quad \{53b\} $$

In order to complete the finite element formulation requires the derivatives of material relations with respect to the nodal displacements. Using the chain rule:

$$\frac{\partial P_R}{\partial u_1} = -\frac{\partial P_R}{\partial u_2} = -\frac{{}^I J_R}{H} \qquad \{54a\}$$

$$\frac{\partial P_\theta}{\partial u_1} = \frac{\partial P_\theta}{\partial u_2} = \frac{J_\theta^*}{2R} \qquad \{54b\}$$

where:

$${}^I J_R = K_2(K_1 - P_R)$$

$$J_\theta^* = \frac{J_\theta J_{CMD}}{J_{CMD} - J_\theta \nu_{CMD\theta}^2}$$

Inserting these derivatives into the stiffness terms {50} completes the nonlinear finite element formulation of a typical element for the material modal *I*. Again for the sake of simplicity constant strain is assumed throughout the element and setting $\eta = 0$ yields the following forms for the element tangent stiffness matrix and element force vector:

$${}^I K^e = \begin{bmatrix} \frac{R\,{}^I J_R}{H} + \frac{H J_\theta^*}{4R} & -\frac{R\,{}^I J_R}{H} + \frac{H J_\theta^*}{4R} \\ sym. & \frac{R\,{}^I J_R}{H} + \frac{H J_\theta^*}{4R} \end{bmatrix}$$

$${}^I F^e = \begin{bmatrix} P_R R - (P_\theta + T_w)\frac{H}{2} \\ -P_R R - (P_\theta + T_w)\frac{H}{2} \end{bmatrix}$$

NUMERICAL PROCEDURE

The finite element formulations developed above can now be implemented into wound roll algorithms. Since the tangent stiffness matrices are 2x2 and symmetric the usual finite element assemblage procedure results in a very compact form, especially when stored in rectangular matrices. The wound roll model will include the core structure. The core structure is easily modeled with stiffness terms similar to the web structure but with different material constants. In calculations herein the core is considered to be composed of a linear orthotropic material. The general frame work of algorithm is shown in a flow chart in Figure 3. The key for the algorithm is the definition of a state during calculation. State *(j,i)* in the algorithm is defined as the state (configuration, material properties) of the system for $i^{th.}$ iteration step during the addition of the $j^{th.}$ layer. After convergence to a desired accuracy is obtained for the addition of a layer the code determines whether there is enough space for the next layer prior to achieving the final wound roll radius. If there is adequate space then the code calculates the initial coordinates of a new layer and places it at the top of current configuration and the iteration procedure will start again. A linear form of the nonlinear model can be obtained if the iteration decision is omitted. In this case for every lap there will be only single

iteration. In fact for hard materials with low radial compressibility the nonlinear code indeed executes only for a few iterations prior to convergence. For very soft materials there may be no convergence so there is a limit ($i_{max} = 100$) on the iteration counter i. If the code attains this limit the process will be terminated. The material model proposed herein (the model with left superscript *I*) exhibits a much more stable and computationally efficient character while solving the winding problem for some imaginary very soft materials. The second model (model *II*) which is sharing the same compact finite element formulation but based on Arola's material assumptions requires iteration limiters for avoiding infinite loops.

RESULTS AND DISCUSSION

In this section the results of the nonlinear models (model *I* and *II*) (which are denoted as PK1 and PK2 in the graphs), the linear models (which are denoted as LINEAR and LINEAR TL), Benson's large deformation model and Hakiel's classic model will be compared. The results from models will also be compared with experimental results which were collected in winding tests of spun-bond nonwoven polypropylene and bath tissue webs that are fine examples of webs with very high radial compressibility. Finally results were compared with the previous experimental work done on newsprint by Good et al [2]. Before the comparison can precede the details of linear models and Benson's material model require review.

The results for simple linear models which are based on the same compact finite element formulation but derived for small strain assumptions will also be compared. Model results with a "LINEAR TL" tag corresponds to small strain version of PK1 and it can be easily obtained if the actual PK1 allowed iterating only for once per model layer. Here TL stands for "tension loss" which is a feature built in the model instinctively because of the pre-stress formulation. In this situation the final tension of a winding layer will be lower than the web line stress as expected. The model with "LINEAR" tag is basically same with the "LINEAR TL" but it iterates for the winding layer's tension in order to obtain the web line tension level. In this situation the final tension of a winding layer will be equal to the web line stress after iteration. Since the material properties are kept constant during addition of a layer the "LINEAR" model needs only one solution and than a factor can be computed such that when multiplied with incremental strains and stresses desired configuration can be obtained.

In his study Benson used true strain with the Cauchy stresses. Benson started with Pfeiffer's famous radial material model:

$$P_R^{Benson} = K_1\left(e^{K_2\varepsilon_R} - 1\right) \qquad \{55\}$$

Here P_R^{Benson} and ε_R are the compressive Cauchy stress and compressive linear strain in radial direction. Using the initial and current thickness (H and h respectively) the linear strain is given as:

$$\varepsilon_R = \frac{H - h}{H} \qquad \{56\}$$

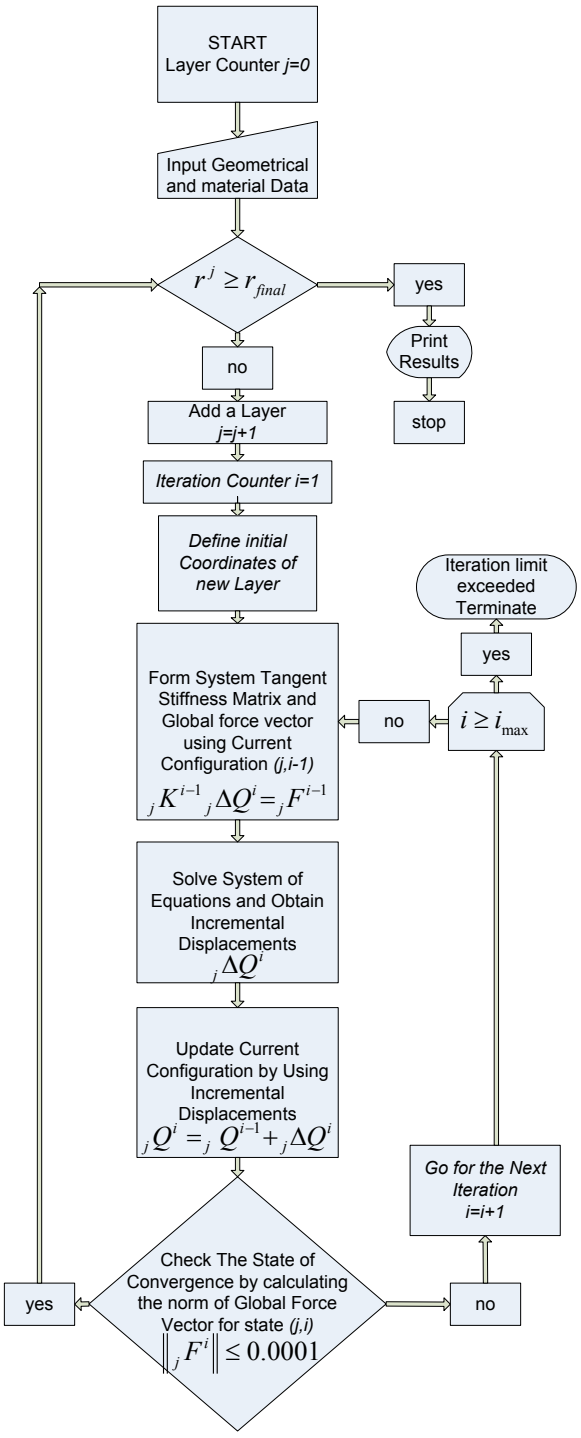

Figure 3 – Flow Chart of Nonlinear Codes

Benson assumed a similar radial material law such that:

$$P_R^{Benson} = \alpha\left(e^{\beta\varepsilon_R^{NL}} - 1\right) \quad \{57\}$$

where α and β are material constants Benson employed instead of K_1 and K_2 because of his choice of strain measure. Here ε_R^{NL} is the true strain and it is given as:

$$\varepsilon_R^{NL} = \ln\left[\frac{H}{h}\right] \quad \{58\}$$

Inserting the true strain expression and after algebraic operations Benson obtained:

$$P_R^{Benson} = \alpha\left(\left(\frac{h}{H}\right)^{-\beta} - 1\right) \quad \{59\}$$

Benson's material model in the tangential direction is the usual small strain material model. He also omitted the Poisson ratios by arguing that they are small. His formulation assumed plane stress conditions so there is no coupling between the CMD and θ directions either. The relation between K_1, K_2 and α, β does not allow any analytical solution and Benson did not propose any method to obtain α, β based upon known values of K_1 and K_2. One solution would be to perform stack compression experiments and curve fit with the relation written in terms of ε_R^{NL} which involves α and β. This is not practical since the K_1, K_2 type measurement has been adapted widely in radial modulus characterization so a numerical conversion algorithm was developed. The development begins by defining the inverse of the compaction ratio of a stack of material which has an initial thickness H:

$$y = \frac{H}{h} \quad \{60\}$$

where h is the thickness under the pressure level P^{SCT}. The superscript SCT stands for Stack Compression Test. For a given material the relation between P^{SCT} and y is known if K_1 and K_2 are known for that material:

$$P^{SCT} = K_1(e^{K_2\left(1-\frac{1}{y}\right)} - 1) \quad \{61\}$$

Taking the derivative of this expression {59} relation with respect to *y* yields:

$$\frac{\partial P^{SCT}}{\partial y} = \left(P^{SCT}\right)' = \frac{K_2K_1(e^{K_2\left(1-\frac{1}{y}\right)})}{y^2} \quad \{62\}$$

This relation can be used to produce *n* data points by defining y_i : $i^{th.}$ step of compaction:

$$y_i = \frac{1}{\overline{h}_i} \qquad \{63\}$$

where $\overline{h}_i$ is the $i^{th.}$ normalized stack height. It can be given as:

$$\overline{h}_i = 1 - (i-1)/100 \qquad \{64\}$$

The $i^{th.}$ derivative of the compressive pressure $\left(P^{SCT}\right)'_i$ can be obtained which corresponds to the normalized stack height $\overline{h}_i$ by substituting y_i into expression {62}:

$$\left(P^{SCT}\right)'_i = \frac{K_2 K_1 (e^{K_2\left(1-\frac{1}{y_i}\right)})}{y_i^2} \qquad \{65\}$$

This is repeated for *i = 1* to *n* and thus *n* data points are obtained:

$$\left\{ y_i, \left(P^{SCT}\right)'_i \right\} \text{ for } i=1,2,\ldots,n \qquad \{66\}$$

The counterpart relation for Benson's model is:

$$P_{SCT} = \alpha(y^{\beta} - 1) \qquad \{67\}$$

If the derivative is taken as before:

$$\frac{\partial P^{SCT}}{\partial y} = \left(P^{SCT}\right)' = \alpha\beta(y)^{\beta-1} \qquad \{68\}$$

A given functional relation written in terms of known K_1 and K_2 constants has been discretized in order to obtain data points for a least square fit of a functional relation written in terms of α and β which are unknown. Taking the logarithms of both sides yields:

$$\ln\left[\left(P^{SCT}\right)'\right] = \ln[\alpha\beta] + (\beta - 1)\ln[y] \qquad \{69\}$$

Now linear regression can be employed over the $\ln\left[\left(P^{SCT}\right)'\right]$ and $\ln[y]$terms to obtain Benson's material model coefficients β and α:

$$\beta = \frac{\left(\sum_{i=1}^{n} i\right)\left(\sum_{i=1}^{n} \ln\left[\left(P^{SCT}\right)'_i\right]\ln[y_i]\right) - \left(\sum_{i=1}^{n} \ln[y_i]\right)\left(\sum_{i=1}^{n} \ln\left[\left(P^{SCT}\right)'_i\right]\right)}{\left(\sum_{i=1}^{n} i\right)\left(\sum_{i=1}^{n} \ln[y_i]^2\right) - \left(\sum_{i=1}^{n} \ln[y_i]\right)^2} + 1 \qquad \{70a\}$$

$$\alpha = \frac{1}{\beta} Exp\left\{\frac{\left[\left(\sum_{i=1}^{n} \ln\left[\left(P^{SCT}\right)'_i\right]\right) - (\beta - 1)\left(\sum_{i=1}^{n} \ln[y_i]\right)\right]}{\left(\sum_{i=1}^{n} i\right)}\right\} \qquad \{70b\}$$

Both models were coded. The stresses presented for the models developed here are the Cauchy stresses since they are the actual stresses measured. For the 1st Piola Kirchoff radial stresses the Cauchy stresses are calculated as:

$$^{I}\sigma_R = \frac{\overline{R}}{\overline{r}} P_R \qquad \{71a\}$$

From the 2nd Piola Kirchoff radial stresses the Cauchy stresses are calculated as:

$$^{II}\sigma_R = \frac{\overline{R}h}{\overline{r}H} S_R \qquad \{71b\}$$

The results are calculated for plane stress case by simply taking the in plane ratio zero. This is done in order to compare with the Benson's and Hakiel's models which were developed for plane stress case. In the charts that follow the Cauchy stresses are plotted versus the final radial positions of layers ($\overline{r}$). The first comparison was performed on a spun-bond non-woven polypropylene material which was 0.152 mm in thickness. The geometric and web material data are provided in Table 1. The test and model results are shown for web line stress level (T_w) of 115 KPa in Figure 4.The pressure data was collected in all cases by winding in pull tabs that extended over the width of the roll and protruded out both sides of the roll. These tabs consist of steel shim enveloped in brass shim to provide a low coefficient of friction. The tabs were inserted in stacks of the non-woven and tissue web. The stacks were subjected to varied pressure and the force required to cause the steel shim to slip within the brass shim was measured. In this way calibration curves were developed for each pull tab. The pull tabs were then wound into test rolls and after winding completed the force required to cause each pull tab to slip was measured and from the calibration charts the pressure was then known at that roll radius.

Tests and simulations were also conducted for a bath tissue which was 0.182 mm in thickness. Note the inputs required to execute the models are provided in Table 2. Also note that the tests and simulations were conducted for two winding tensions. Results for a web line tension of 92.4 KPa are presented in Figure 5 and results for a web line tension of 59.2 KPa are presented in Figure 6.

Core inner radius	1.27 cm	J_{CMD}	16550 KPa
Core outer radius	5.08 cm	J_{core}	6.9 10^8 KPa
Roll final radius	24.1 cm	ν_{core}	0.3
K_1	1.32 KPa	α	2.25 KPa
K_2	13.39	β	9.6
J_θ	55160 KPa	T_w	115 KPa

Table 1 – Material and geometric properties for Spun-bond Non-Woven Polypropylene

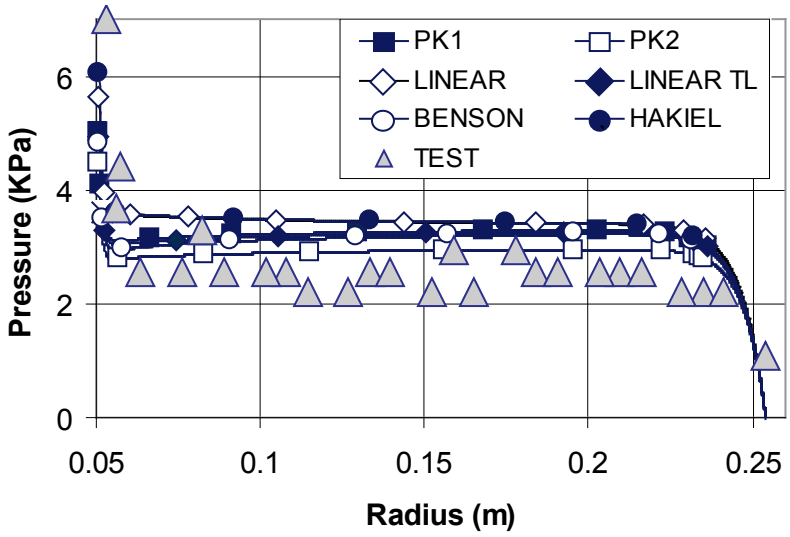

Figure 4 – Radial Pressures for Spun-bond Non-Woven – T_w=*115* KPa

Core inner radius	1.27 cm	J_{CMD}	3337 KPa
Core outer radius	4.45 cm	J_{core}	6.9 10^8 KPa
Roll final radius	19 and 22.9 cm	ν_{core}	0.3
K_1	0.258 KPa	α	0.44
K_2	13.474	β	9.67
J_θ	3337 KPa	T_w	59.2 and 92.4 KPa

Table 2 – Material and geometrical properties for Bath Tissue

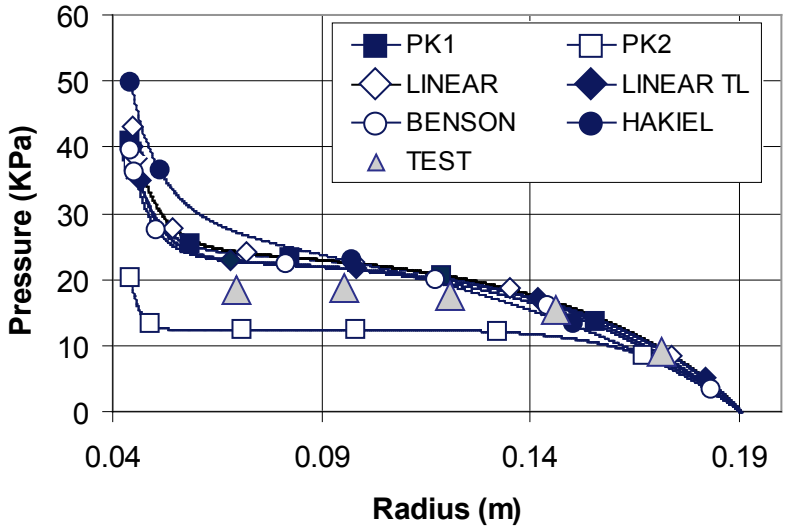

Figure 5 – Radial Pressures for Bath Tissue– T_w=*92.4* KPa

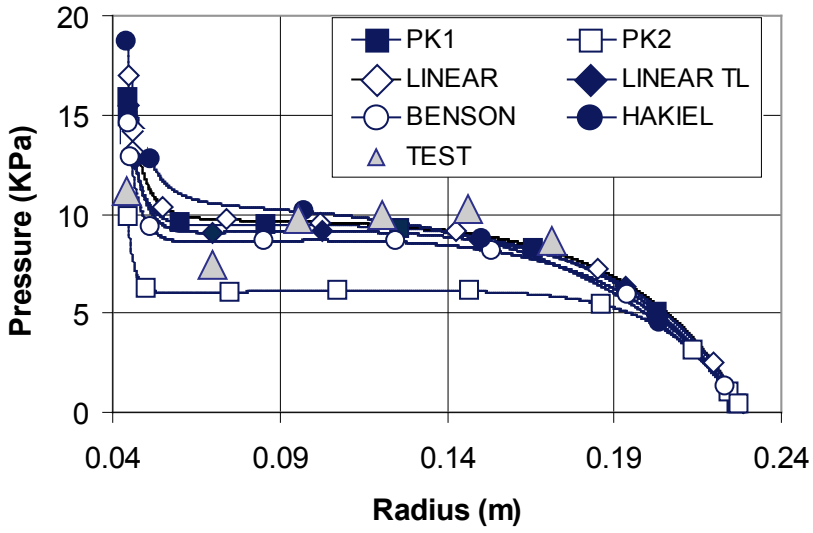

Figure 6 – Radial Pressures for Bath Tissue– T_w=*59.2* KPa

The material and geometrical data for the newsprint which was 0.071 mm in thickness is given in Table 3. Newsprint results are shown for two levels of web line stress: 5.17 and 3.45 MPa in Figures 7 and 8 respectively.

Core inner radius	1 cm	J_{CMD}	3.37GPa
Core outer radius	4.45 cm	J_{core}	6.9 10^8 KPa
Roll final radius	13.35 cm	ν_{core}	0.3
K_1	1.175 KPa	α	1.54 KPa
K_2	45.14	β	39.72
J_θ	3.37 GPa	T_w	3.45, 5.17 MPa

Table 3 – Material and geometrical properties for Newsprint

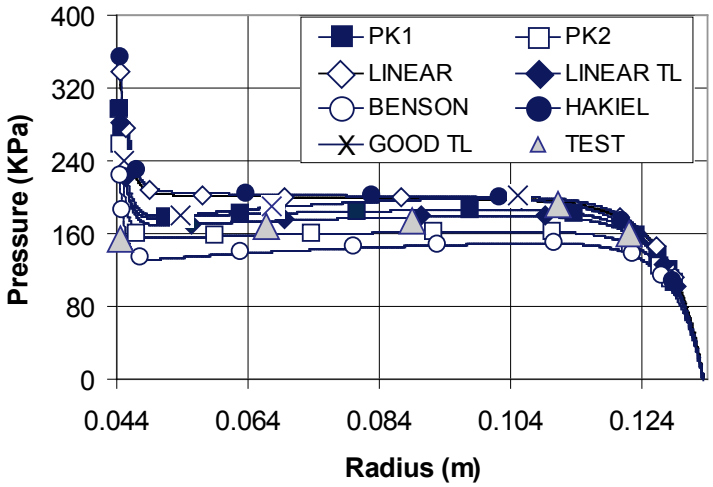

Figure 7 – Radial Pressures for Newsprint– T_w=*5.17.* MPa

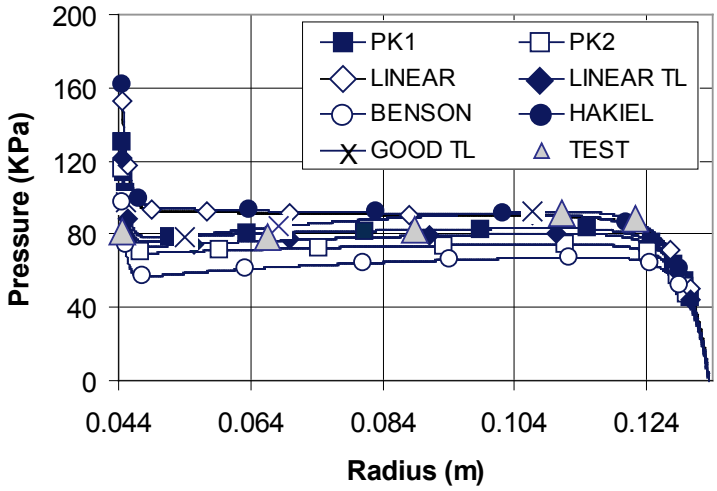

Figure 8 – Radial Pressures for Newsprint– T_w=*3.45* MPa

Mean absolute error tables have been produced for the cases shown here in order to clearly understand the models prediction capabilities in comparison to the test data. Tables 4, 5 and 6 are calculated for the spun-bond non-woven, the bath tissue and newsprint, respectively.

Spun-bond	Mean Absolute Error (KPa)
Models	Tw=115. (KPa)
PK1	0.124
Linear	0.139
Linear TL	0.122
PK2	0.094
Benson	0.120
Hakiel	0.139

Table 4 – Mean Absolute Error for Spun-bond Non-Woven

Bath Tissue	Mean Absolute Error (kPa)	
Models	Tw= 92.4 (kPa)	Tw=59.2 (kPa)
PK1	0.653	0.140
Linear	0.701	0.132
Linear TL	0.585	0.152
PK2	0.610	0.455
Benson	0.530	0.189
Hakiel	0.689	0.180

Table 5 – Mean Absolute Error for Bath Tissue

Newsprint	Mean Absolute Error (kPa)	
Models	Tw= 3.45 (mPa)	Tw=5.17 (mPa)
PK1	8.81	13.0
Linear	19.7	51.5
Linear TL	13.6	30.5
PK2	16.7	34.0
Benson	17.0	31.2
Hakiel	22.0	54.8
Good TL	12.5	41.9

Table 6 – Mean Absolute Error for Newsprint

In Table 6 we have also included results from Good's tension loss model (Good TL) [2].

CONCLUSIONS

Based on comparison of error levels from tables from all the nonlinear models for all web materials studied it cannot be said that one nonlinear model is superior to another. From Table 4 it is seen that PK2 is best for Spun-bond Nonwoven , from Table 5 its is seen that PK1 and Benson's models predicted better for bath tissue and finally from Table 6 it is clear that PK1 works better for newsprint. It can be concluded that all these nonlinear models produced similar results.

An important question would be why do the results of the nonlinear models and the linear model that accounts for tension loss agree so well? When a layer of web material is added to the outside of a winding roll the majority of the deformation occurs in an outer few laps. Both the nonlinear Model I and the linear model are pre-stress formulations that allow the loss of tension in the outer layer reported by Good et al [2]. It must be concluded that the interaction between stress and deformation in the layers beneath the outer lap are inconsequential on the final stress or pressure distributions in the roll. Still intriguing are the levels of radial strain wound into these rolls. To demonstrate the total radial strain for the spun-bond non-woven, computed using the nonlinear Model I, is shown in Figure 9. As shown these strains are much in excess of the 1% that is conventionally held as the limit for linear small strain analyses. Although it is possible that nonlinear models may show benefit for materials with yet lower K_1 and K_2 values it must also be said that the spun-bond non-woven and tissue webs for which results were reported herein have some of the lowest K_1 and K_2 values the authors have ever witnessed among a host of web materials. So it is unknown if yet more compressible webs exist that would require the use of a nonlinear wound roll model. That being said all the wound roll models discussed herein account for material nonlinearity.

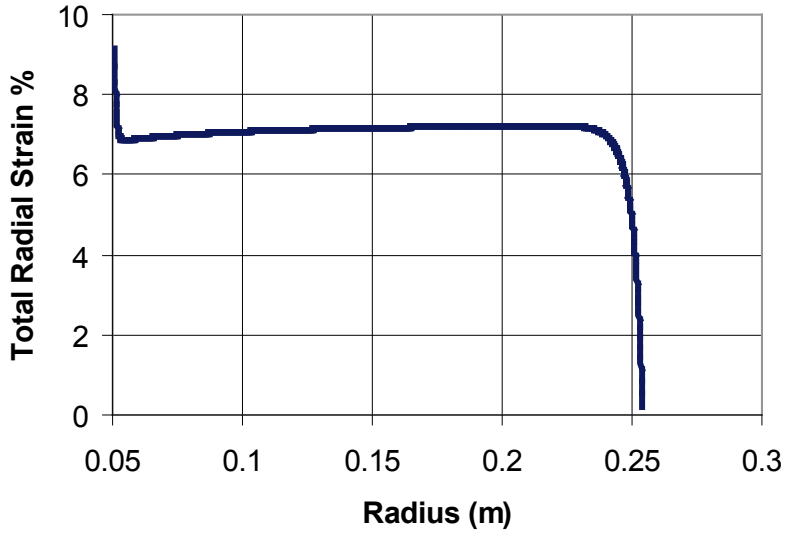

Figure 9 – Total Radial Strain from Model I for Spun-Bond Non-Woven – T_w=*115* KPa

The findings herein are important as wound roll models have already evolved to 2D axisymmetric codes such that the effects of thickness and length nonuniformities can be examined. This has caused a dramatic increase in problem size and if nonlinearity was important iteration would be required and huge investments of computation time would

be required to solve problems where the web compressibility was high. The finding that linear models that account for tension loss (such as the pre-stress axisymmetric code - described herein as Linear TL) produce accurate results for even these highly compressible materials will help to greatly reduce computational time in the 2D codes.

REFERENCES

1. Hakiel, Z., "Nonlinear model for wound roll stresses," Tappi Journal, 1987.
2. Good, J. K., Pfeiffer, J. D., and Giachetto, R. M., "Losses in Wound-on Tension in the Center Winding of Wound Rolls," Proceedings of Web Handling Symposium, ASME, Applied Mechanics Division, AMD-Vol. 149, 1992, pp.1-11.
3. Benson R. C., "A Nonlinear Wound Roll Model Allowing for Large Deformation," Journal of Applied Mechanics, Vol. 62, 1995, pp.853-859.
4. Pfeiffer J. D., "Internal Pressures in a Wound Roll of Paper," Tappi Journal, Vol. 49,1966, pp.342-347.
5. Good, J. K., "The Abilities and Inabilities of Wound Roll Models to Predict Winding Defects," Keynote Presentation – Proceedings of the Eighth International Web Handling Conference, Oklahoma State University, Stillwater, Oklahoma, 2005.
6. Arola, K. and von Hertzen R., "Two-Dimensional Axisymmetric Winding Model for Finite Deformation," Computational Mechanics, Vol. 40, 2007, pp.933-947.

Large Deformation Winding Models

C. Mollamahmutoglu & J. K. Good, Oklahoma State University, USA

Name & Affiliation	**Question**
Balaji Kandadai, Kimberly-Clark Corporation	You have shown results where K_2 is very low and hence the radial modulus is small. Have you tried to model webs that have really low machine direction modulus as well as low K_2 values?
Name & Affiliation	**Answer**
C. Mollamahmutoglu, Oklahoma State University	For bath tissue the MD modulus is very low, it is about 3.337 MPa. The results we have shown are for real webs with low radial and machine direction modulus. We elected to show results for the newsprint because it was used in two previous publications regarding tension loss and nonlinear wound roll models. We then produced results for the bath tissue and the non-woven webs because these were the lowest modulus webs available and should provide a true test of the value of a nonlinear model. Certainly it would be possible to run these models for imaginary webs with even smaller modulus values than those studied thus far. We elected to show results for existing webs.
Name & Affiliation	**Comment**
J. K. Good, Oklahoma State University	If you look at the spun-bond materials in Table 1, the K_2 values are not all that different than the bath tissue in Table 2. The big difference between the spun-bond and the bath tissue is that in the MD modulus J_θ are really quite a bit different. This is part of the reason we showed the results for these two materials. Why do the linear models which employ tension loss work so well in these cases for these materials which are some of the lowest K_2 that we have measured? Part of my explanation for this is that these materials are incapable of reacting much web tension prior to failure. If you could subject these webs to greater winding tension without failing them, perhaps you would see a greater benefit of the nonlinear models. If webs are developed that have low MD and radial modulus and can be subjected to high winding tension we could see benefit from the nonlinear winding models. My experience is that these properties are mutually exclusive however.
Name & Affiliation	**Question**
Dilwyn Jones, Emral Ltd.	You have shown that the linear and nonlinear models are similar in the predictions for the pressure, have you looked at the circumferential stresses to see if they are similar?
Name & Affiliation	**Answer**
C. Mollamahmutoglu, Oklahoma State University.	Yes, we looked at them and yes they are similar.

Name & Affiliation	Question
Balaji Kandadai, Kimberly-Clark Corporation	It appears the linear tension loss model accounts for the majority of the nonlinearity in the winding roll. Since this type of model produces results that are essentially the same as the nonlinear models does this mean the nonlinear behavior of the inner layers of the wound roll is small and inconsequential?
Name & Affiliation	**Answer**
C. Mollamahmutoglu, Oklahoma State University	Yes, you are correct.